

Effect of aging on muscle mitochondrial substrate utilization in humans

Kitt Falk Petersen^a, Katsutaro Morino^{a,b}, Tiago C. Alves^a, Richard G. Kibbey^a, Sylvie Dufour^b, Saki Sono^{a,b}, Peter S. Yoo^c, Gary W. Cline^a, and Gerald I. Shulman^{a,b,d,1}

^aDepartment of Internal Medicine, Yale University School of Medicine, New Haven, CT 06520; ^bHoward Hughes Medical Institute, Yale University School of Medicine, New Haven, CT 06520; ^cDepartment of Surgery, Yale University School of Medicine, New Haven, CT 06520; and ^dDepartment of Cellular and Molecular Physiology, Yale University School of Medicine, New Haven, CT 06520

Contributed by Gerald I. Shulman, July 28, 2015 (sent for review March 30, 2015; reviewed by Robert Harris and Roy Taylor)

Previous studies have implicated age-associated reductions in mitochondrial oxidative phosphorylation activity in skeletal muscle as a predisposing factor for intramyocellular lipid (IMCL) accumulation and muscle insulin resistance (IR) in the elderly. To further investigate potential alterations in muscle mitochondrial function associated with aging, we assessed basal and insulin-stimulated rates of muscle pyruvate dehydrogenase (V_{PDH}) flux relative to citrate synthase flux (V_{CS}) in healthy lean, elderly subjects and healthy young body mass index- and activity-matched subjects. V_{PDH}/V_{CS} flux was assessed from the ^{13}C incorporation from of infused [$1-^{13}C$] glucose into glutamate [$4-^{13}C$] relative to alanine [$3-^{13}C$] assessed by LC-tandem MS in muscle biopsies. Insulin-stimulated rates of muscle glucose uptake were reduced by 25% ($P < 0.01$) in the elderly subjects and were associated with ~70% ($P < 0.04$) increase in IMCL, assessed by 1H magnetic resonance spectroscopy. Basal V_{PDH}/V_{CS} fluxes were similar between the groups (young: 0.20 ± 0.03 ; elderly: 0.14 ± 0.03) and increased approximately threefold in the young subjects following insulin stimulation. However, this increase was severely blunted in the elderly subjects (young: 0.55 ± 0.04 ; elderly: 0.18 ± 0.02 , $P = 0.0002$) and was associated with an ~40% ($P = 0.004$) reduction in insulin activation of Akt. These results provide new insights into acquired mitochondrial abnormalities associated with aging and demonstrate that age-associated reductions in muscle mitochondrial function and increased IMCL are associated with a marked inability of mitochondria to switch from lipid to glucose oxidation during insulin stimulation.

glucose oxidation | fat oxidation | LC-tandem MS | respiratory quotient | pyruvate dehydrogenase

Impaired glucose tolerance and type 2 diabetes affect ~40% of all Americans over the age of 65, yet the pathogenesis of this age-associated deterioration in glucose metabolism is poorly understood (1–4). In this regard, previous studies demonstrated that aging is associated with muscle insulin resistance, increased intramyocellular lipid (IMCL) content, and reductions in basal rates of muscle mitochondrial oxidative and phosphorylation activity (5). These results led to the hypothesis that age-associated reductions in muscle mitochondrial function may be an important predisposing factor in the elderly predisposing them to develop increased ectopic lipid deposition in skeletal muscle, muscle insulin resistance, and type 2 diabetes (5–9).

To further examine the impact of aging on basal and insulin-stimulated muscle mitochondrial function, we developed and applied a novel LC-tandem MS (LC-MS/MS) method to directly estimate relative rates of muscle mitochondrial pyruvate dehydrogenase flux (V_{PDH}) and citrate synthase flux (V_{CS}) in vivo under both basal and insulin-stimulated conditions. Relative rates of mitochondrial V_{PDH} to V_{CS} fluxes were assessed by measuring the relative ^{13}C enrichments of [$4-^{13}C$] glutamate to [$3-^{13}C$] alanine in muscle biopsies obtained before and after a hyperinsulinemic-euglycemic clamp using [$1-^{13}C$] glucose (10). Using this approach, we observed that aging is associated with a

marked inability for muscle mitochondria to switch from lipid to glucose oxidation during insulin stimulation.

Results

Oral Glucose Tolerance Test. Fasting plasma glucose concentrations were higher in the elderly subjects than in the young control subjects (Table 1). Fasting plasma concentrations of insulin, high-molecular-weight (HMW) adiponectin, C-reactive protein, and leptin were similar between the two groups (Table 1). All subjects had normal glucose tolerance following ingestion of the glucose, although plasma concentrations of both glucose and insulin during the test were significantly higher in the elderly than the young control subjects (Fig. 1*A* and *B*). Fasting plasma nonesterified fatty acid concentrations were similar in both groups and suppressed by ~75% in both groups during the glucose tolerance test (Fig. 1*C*).

Intramyocellular Lipid Content. IMCL content, measured by localized 1H magnetic resonance spectroscopy (MRS) of the soleus muscle, was 73% higher in the elderly subjects compared with the young subjects (Table 1).

Hyperinsulinemic–Euglycemic Clamp Studies with Muscle Biopsies to Assess Insulin Stimulation of AKT2 and Mitochondria Density. During the hyperinsulinemic-euglycemic clamp study, plasma concentrations of insulin were raised to 40 ± 3 and 44 ± 3 $\mu U/mL$ throughout the clamp period, and plasma glucose concentrations were maintained at 5.5 ± 0.1 and 5.6 ± 0.1 mmol/L in the elderly and young subjects, respectively. Basal rates of endogenous glucose production were similar in the young [1.84 ± 0.04 mg/(kg·min)] and

Significance

Approximately 40% of Americans over the age of 65 suffer from impaired glucose tolerance or type 2 diabetes; however, the pathogenesis of aging-associated reductions in glucose metabolism is poorly understood. Aging is associated with muscle insulin resistance, increased intramyocellular fat content, and reductions in rates of muscle mitochondrial activity. To further examine the potential role of age-associated alterations in mitochondrial metabolism, we applied a novel method to assess muscle specific rates of mitochondrial glucose and fat oxidation and demonstrate that aging is also associated with a marked inability of mitochondria to switch from lipid to glucose oxidation on insulin stimulation, which may further contribute to dysregulated glucose and lipid metabolism in the elderly.

Author contributions: K.F.P., K.M., R.G.K., and G.I.S. designed research; K.F.P., K.M., T.C.A., R.G.K., S.D., S.S., P.S.Y., and G.W.C. performed research; T.C.A. and R.G.K. contributed new reagents/analytic tools; K.F.P., K.M., T.C.A., R.G.K., S.D., G.W.C., and G.I.S. analyzed data; and K.F.P., K.M., T.C.A., R.G.K., G.W.C., and G.I.S. wrote the paper.

Reviewers: R.H., Indiana University School of Medicine; and R.T., University of New Castle.

The authors declare no conflict of interest.

Freely available online through the PNAS open access option.

¹To whom correspondence should be addressed. Email: gerald.shulman@yale.edu.

Table 1. Anthropomorphic and metabolic characteristics in young and elderly subjects

Anthropomorphic and metabolic characteristics	Young subjects (n = 15)	Elderly subjects (n = 15)	P value
Age (years)	27 ± 2	69 ± 1	
BMI (kg/m ²)	23.3 ± 0.5	24.5 ± 0.5	NS
Lean body mass (%)	56.6 ± 1.9	54.5 ± 2.5	NS
Activity (miles/d)	3.9 ± 0.5	3.2 ± 0.4	NS
IMCL (%)	0.80 ± 0.10	1.38 ± 0.22	<0.04
Insulin sensitivity index (ISI)	5.4 ± 0.3	4.1 ± 0.3	0.007
Fasting plasma glucose (mmol/L)	4.9 ± 0.1	5.4 ± 0.4	0.020
Fasting plasma insulin (μU/mL)	9 ± 1	10 ± 1	NS
Plasma leptin (ng/mL)	5.8 ± 1.0	6.2 ± 1.1	NS
Plasma HMW adiponectin (μg/mL)	7.5 ± 0.9	9.8 ± 1.0	NS
Plasma C-reactive protein (μg/mL)	0.56 ± 0.23	1.06 ± 0.62	NS
Rates of basal whole body energy expenditure (kcal/24 h)	1,670 ± 52	1,423 ± 48	<0.002
Fasting RQ	0.77 ± 0.02	0.82 ± 0.02	<0.05

the elderly subjects [1.97 ± 0.09 mg/(kg·min); $P =$ not significant (NS)] and almost completely suppressed in both groups during the hyperinsulinemic-euglycemic clamp [young: 0.25 ± 0.06 mg/(kg·min) vs. elderly: 0.11 ± 0.08 mg/(kg·min); $P =$ NS]. Insulin-stimulated rates of peripheral glucose uptake were reduced by 25% in the elderly subjects compared with the young subjects [6.4 ± 0.5 vs. 4.5 ± 0.4 mg/(kg·min); $P < 0.01$]. This reduction in insulin-stimulated peripheral glucose metabolism could be mostly attributed to a 40% reduction in nonoxidative glucose disposal in the elderly subjects [young: 5.3 ± 0.4 vs. elderly: 3.0 ± 0.7 mg/(kg·min); $P < 0.002$]. Furthermore, this reduction in insulin-stimulated rates of glucose metabolism in the elderly subjects was associated with a 40% reduction in insulin activation of Akt2 in skeletal muscle of the elderly subjects compared with the young subjects ($P = 0.004$; Fig. 2).

Basal rates of glycerol turnover were similar in the elderly subjects (0.23 ± 0.03 μmol/kg·min) and young subjects (0.26 ± 0.03 μmol/kg·min; $P =$ NS) and were suppressed similarly in the two groups during the hyperinsulinemic-euglycemic clamp (elderly: $62 \pm 3\%$ and young: $55 \pm 3\%$; $P =$ NS).

Mitochondrial density in the muscle samples, assessed by electron microscopy, tended to be lower in the elderly subjects ($2.02 \pm 0.24\%$) compared with the young subjects ($2.30 \pm 0.24\%$; $P = 0.34$); however, this difference was not significant.

Hyperinsulinemic–Euglycemic Clamp Studies with Muscle Biopsies to Assess V_{PDH}/V_{CS} Flux. A subgroup of young and elderly subjects underwent a second hyperinsulinemic-euglycemic clamp study combined with muscle biopsies before and at the end of the clamp to assess the effects of aging on basal and insulin-stimulated V_{PDH}/V_{CS} flux. Plasma concentrations of insulin were raised to 83 ± 4 and 70 ± 6 μU/mL ($P =$ NS), and plasma glucose concentrations were maintained throughout the clamp period at 5.3 ± 0.1 and 5.5 ± 0.1 mmol/L ($P =$ NS) in the elderly and young subjects, respectively.

In the elderly subjects, rates of insulin-stimulated peripheral glucose uptake [young: 11.2 ± 0.5 vs. elderly: 6.8 ± 1.2 mg/(kg·min); $P = 0.001$] were reduced by 40% compared with the young subjects.

Relative fluxes of V_{PDH}/V_{CS} flux in skeletal muscle following an overnight fast were similar in the two groups [young: 0.20 ± 0.03 vs. elderly: 0.14 ± 0.03 ; $P =$ NS; Fig. 3]. During the hyperinsulinemic-euglycemic clamp, muscle V_{PDH}/V_{CS} flux increased by threefold in the young subjects to 0.55 ± 0.04 ($P = 0.001$ vs. basal). In contrast, rates of insulin-stimulated muscle V_{PDH}/V_{CS} flux did not change in the elderly subjects following the hyperinsulinemic-euglycemic clamp, resulting in a marked defect in insulin-stimulated increases in V_{PDH}/V_{CS} flux in the elderly

subjects compared with the young subjects (elderly: 0.18 ± 0.02 ; $P = 0.0002$ vs. young; Fig. 3).

Indirect Calorimetry. The basal respiratory quotient (RQ) value was higher in the elderly subjects than in the young subjects (Table 1). Basal rates of whole body energy expenditure were also 15% lower in the elderly subjects compared with the young subjects (Table 1).

Discussion

Previous studies demonstrated that healthy lean elderly subjects had a marked impairment in insulin-stimulated muscle glucose metabolism, which was associated with increased IMCL content and reduced mitochondrial oxidative-phosphorylation activity in

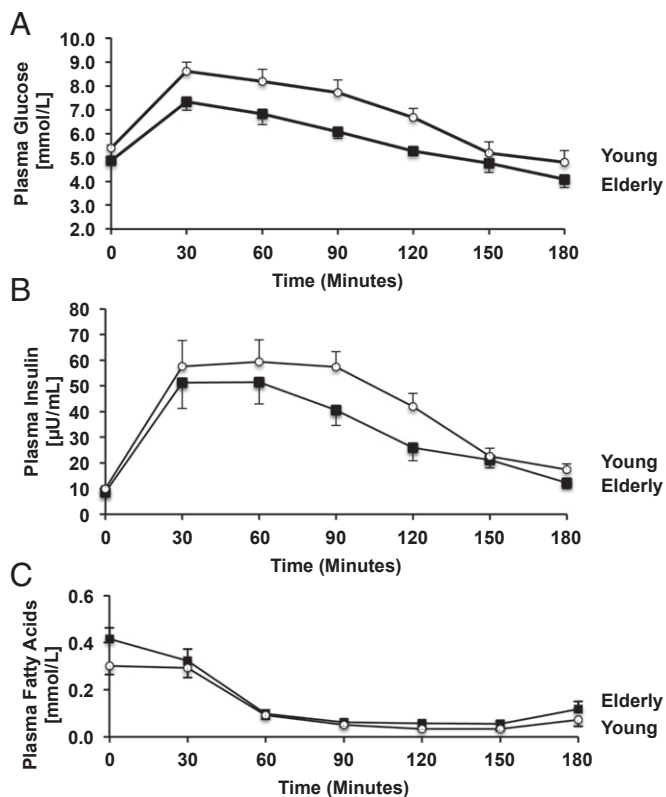


Fig. 1. Mean (\pm SEM) plasma concentrations of glucose (A), insulin (B), and nonesterified fatty acids (C) before and during an OGTT in the young and elderly subjects.

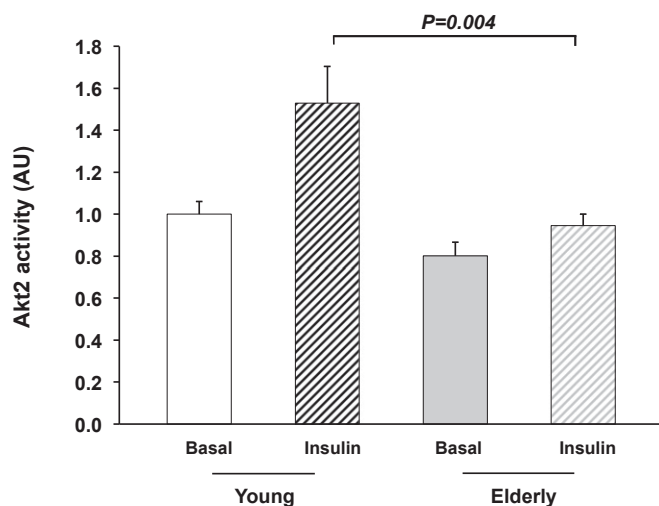


Fig. 2. Muscle Akt2 activity before and after 20 min of insulin stimulation in the young and elderly subjects.

skeletal muscle (5). These results led to the hypothesis that age-associated reductions in muscle mitochondrial function may be an important predisposing factor for ectopic lipid accumulation in skeletal muscle, which in turn would result in defects in insulin signaling and muscle insulin resistance (5, 8, 9). Consistent with this hypothesis, we found that a similar group of healthy lean elderly subjects manifested marked impairment of insulin-stimulated peripheral glucose metabolism, which was associated with increased IMCL content and reduced insulin-stimulated AKT2 activity in skeletal muscle. These results demonstrate that increased IMCL in the elderly is associated with reduced insulin signaling in muscle providing further evidence that intrinsic defects in insulin action in skeletal muscle contribute to whole body insulin in the elderly in addition to age-associated reductions in muscle mass (11).

To gain further insights into the impact of aging on basal and insulin-stimulated muscle mitochondrial function and substrate utilization, we developed and applied a novel LC-MS/MS method to directly estimate relative rates of muscle mitochondrial V_{PDH} flux and V_{CS} flux *in vivo* under both basal and insulin-stimulated conditions. Relative rates of V_{PDH} flux to V_{CS} flux were assessed by measuring the relative ^{13}C enrichments of [4- ^{13}C] glutamate to [3- ^{13}C] alanine, a surrogate for intramyocellular pyruvate, in muscle biopsies obtained before and after a hyperinsulinemic-euglycemic clamp using [1- ^{13}C] glucose as previously described (10).

In contrast to indirect calorimetry, which provides information regarding relative rates of glucose vs. fat oxidation (RQ) in the whole body, our method assesses muscle specific rates of mitochondrial glucose vs. fat oxidation. Previous studies have attempted to assess muscle specific RQ by measuring arteriovenous balances of O_2 and CO_2 concentrations in the leg (12). However, this approach can be affected by the presence of other tissues with different RQ values such as adipose tissue, bone, and skin draining into the vein. Another inherent problem with this approach is its dependency on blood flow. Factors like temperature or hormonal stimulation can affect blood flow and therefore influence the value of RQ obtained (13).

Using our LC-MS/MS approach, we found that, despite a significantly higher whole body RQ in the elderly subjects compared with the young subjects, muscle-specific V_{PDH}/V_{CS} flux was similar (~15%) in the two groups following an overnight fast. These results demonstrate that mitochondria in resting skeletal muscle of both young lean insulin sensitive healthy control subjects

and insulin resistant elderly subjects rely similarly (~85%) on fatty acid oxidation to meet their energy requirements despite the presence of muscle insulin resistance in the elderly. Furthermore, given the higher RQ observed in the elderly, these results demonstrate the inability of whole body calorimetry to adequately reflect relative changes in glucose vs. fat oxidation in skeletal muscle.

On insulin stimulation, we found that V_{PDH}/V_{CS} flux increased approximately threefold in skeletal muscle of the young individuals, reflecting a switch from mostly lipid oxidation to a state where approximately half of the energy derived for mitochondrial metabolism could now be attributed to glucose oxidation. In contrast, we found that this increment in insulin-stimulated V_{PDH}/V_{CS} flux was severely blunted in the muscle of the elderly subjects, reflecting an inability of the muscle to switch from lipid to glucose oxidation during insulin stimulation. Although the mechanism for this inability to increase mitochondrial glucose oxidation on insulin stimulation in the elderly remains unknown, lipid-induced defects in insulin signaling, as reflected by the observed reductions in insulin-stimulated AKT activity in the elderly (8, 14, 15), could explain this abnormality through a substrate push mechanism mediated by reductions of insulin-stimulated glucose transport into the muscle cell.

In summary, these results demonstrate that in addition to reduced rates of mitochondrial oxidative phosphorylation activity aging is also associated with a marked inability of mitochondria to switch from lipid to glucose oxidation on insulin stimulation, which may further contribute to dysregulated glucose and lipid metabolism in the elderly.

Methods

Subjects. Healthy, normal weight elderly individuals ($n = 15$; age: 69 ± 1 y) were recruited by local advertising and prescreened to confirm that they were in excellent health, lean, and nonsmoking. A group of young ($n = 15$; age: 27 ± 2 y) volunteers, who had no family history of diabetes or hypertension, were matched to the elderly subjects for body mass index (BMI), fat mass, and habitual physical activity. All qualifying subjects underwent a complete medical history and a physical examination with blood tests to verify normal blood and platelet counts and concentrations of aspartate aminotransferase, alanine aminotransferase, blood uric acid, cholesterol, and triglycerides, prothrombin time and partial-thromboplastin time. All had a normal birth weight (>2.3 kg) and a sedentary lifestyle, as defined by an activity index questionnaire (16) and by measuring habitual physical activity over 3 consecutive days by step counting using a pedometer (Sportline). Only subjects who were not participating in regular physical activity and had an average daily physical activity of

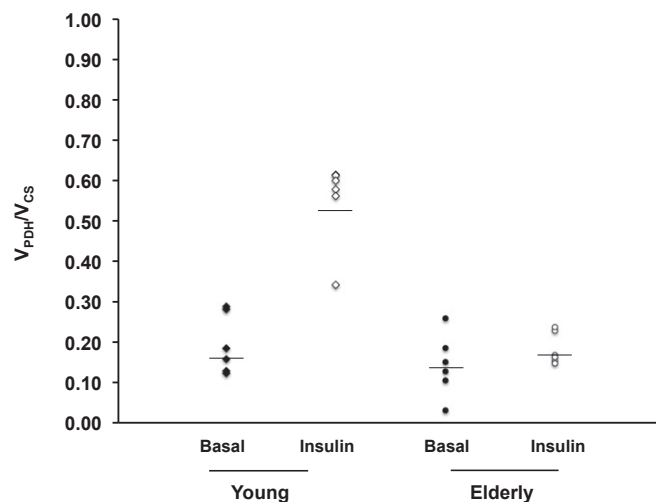


Fig. 3. Basal and insulin-stimulated muscle V_{PDH}/V_{CS} flux as estimated from the [4- ^{13}C] glutamate/[3- ^{13}C] alanine enrichments in muscle tissue of young and elderly subjects before and during a hyperinsulinemic-euglycemic clamp.

less than walking 4.8 km (~10,000 steps) were eligible. The subjects were prescreened with a 3-h oral glucose tolerance test (OGTT) to assure normal glucose tolerance and ^1H MRS studies to measure hepatic triglyceride, and IMCL content (5). The initial insulin sensitivity was calculated from the OGTT plasma glucose and insulin levels and an insulin sensitivity index (ISI) as previously described (17) (Table 1).

All subjects underwent the OGTT to assess glucose tolerance, ^1H MRS measurements of intramyocellular lipid content (IMCL), and study 1 with tracer infusions and a hyperinsulinemic-euglycemic clamp study with muscle biopsies before and after the clamp to assess insulin sensitivity, mitochondrial density, and Akt activity. Due to lack of sufficient tissue Akt, activity was assessed in subgroups of young ($n = 11$) and elderly subjects ($n = 8$) subjects.

In a parallel set of studies, subgroups of the elderly ($n = 6$) and young ($n = 6$) subjects underwent study 2, with a [$1\text{-}^{13}\text{C}$] glucose infusion and a hyperinsulinemic-euglycemic clamp study with muscle biopsies to assess insulin-stimulated $V_{\text{PDH}}/V_{\text{CS}}$ fluxes before and after insulin stimulation as described below. The protocol was approved by the Yale Human Investigation Committee, and written consent was obtained from each subject after the purpose, nature, and potential complications of the studies had been explained.

OGTT. The subjects were admitted to the Yale–New Haven Hospital Research Unit (HRU) at 7:30 AM after fasting from 8:00 PM the evening before. After obtaining height, weight, and body composition, the subjects remained in bed until the end of the study. Twenty minutes after insertion of an antecubital IV, fasting blood samples were collected, the subjects drank a 75-g standard glucose solution (Glucola; Curtis Matheson Scientific), and blood samples were collected every 30 min for the next 3 h. During the tests, the subject completed physical activity questionnaires as previously described (18).

MRS of IMCL Content. On a separate day, localized ^1H MRS spectra of the soleus muscle were acquired on a 4T Biospec Spectrometer (Bruker Instruments) to assess IMCL content as previously described (19).

Body Composition. Fat and lean body mass were determined in all subjects using bioelectrical impedance Tanita Scale Model BC418 (Tanita Corp.), with the subjects in underwear and bare feet as previously described (18).

Diet and Study Preparation. For 3 d before the studies, the subjects were instructed to eat a regular, weight maintenance diet containing at least 150 g of carbohydrate and not to perform any exercise other than normal walking for the 3 d before the study (5). Subjects were admitted to the Yale–New Haven HRU the evening before the clamp study and remained fasting from 10:00 PM until the completion of the study the following day the subjects continued to fast while having free access to regular drinking water until the end of the studies.

Study 1: Hyperinsulinemic–Euglycemic Clamp Studies with Muscle Biopsies to Assess Mitochondrial Density. After an overnight fast, basal rates of glucose and glycerol turnover were assessed after a 3-h primed-continuous infusion of [$6,6\text{-}^2\text{H}_2$]glucose [99% atom percent enriched (APE) concentration: 25 mg/mL] at a rate of 2.10 mg/($\text{m}^2\cdot\text{min}$) and [$^2\text{H}_5$]glycerol (99% APE concentration: 6.9 mg/mL) at a rate of 1.21 mg/($\text{m}^2\cdot\text{min}$). At the end of this baseline period, muscle biopsies were collected for Akt activity and mitochondrial density. The biopsy site was covered with sterile covers. The biopsies were immediately followed by a 3-h hyperinsulinemic-euglycemic clamp with infusion of insulin at a rate of 20 mU/($\text{m}^2\cdot\text{min}$) (U-100 regular insulin; Novo Nordisk) while keeping plasma glucose concentrations constant at euglycemia by a variable infusion of 2.50% APE [$6,6\text{-}^2\text{H}_2$]glucose (5 g/L of a 200-mg/dL dextrose solution; Cambridge Isotopes). After 20 min of insulin stimulation, muscle biopsies were obtained for determination of mitochondrial density and insulin stimulation of Akt activity (20).

Study 2: Hyperinsulinemic–Euglycemic Clamp Studies with Muscle Biopsies to Assess Basal and Insulin-Stimulated $V_{\text{PDH}}/V_{\text{CS}}$ Flux. After an overnight fast, a 2-h infusion of [$1\text{-}^{13}\text{C}$] glucose (388 mmol/L, 99% APE; Cambridge Isotopes) was initiated as a primed/continuous infusion at a low-dose rate of 0.3 mg/($\text{kg}\cdot\text{min}$). At the end of this 2-h period, basal muscle biopsies were collected for measurements of basal ^{13}C enrichments of [$4\text{-}^{13}\text{C}$] glutamate and [$3\text{-}^{13}\text{C}$] alanine, and a 2-h euglycemic-hyperinsulinemic clamp was started with a primed-continuous insulin infusion at a rate of 40 mU/($\text{m}^2\cdot\text{min}$) (U-100 regular insulin; Novo Nordisk) while keeping plasma glucose concentrations constant at euglycemia with a variable infusion of [$1\text{-}^{13}\text{C}$]

glucose (1.11 M, 25% APE; Cambridge Isotopes). During the final 30 min of this hyperinsulinemic-euglycemic clamp, muscle repeat biopsies were obtained for determination of ^{13}C enrichments in [$4\text{-}^{13}\text{C}$] glutamate and [$3\text{-}^{13}\text{C}$] alanine following insulin stimulation.

Muscle Biopsies. Muscle biopsies were collected after the skin over the vastus lateralis muscle was sterily prepared with betadine and 1% lidocaine was injected s.c. A 2-cm incision was made using a scalpel, and a punch muscle biopsy was extracted using suction and a 5-mm Bergstrom biopsy needle (Warsaw). A piece of muscle tissue was dissected with a scalpel and immediately fixed in glutaraldehyde buffer for electron microscopy studies as described below. The remainder of the muscle tissue was blotted, snap frozen, and stored in liquid nitrogen until assay (20).

Indirect Calorimetry. Rates of whole body energy expenditure and RQs were assessed during the last 30 min of the baseline and hyperinsulinemic-euglycemic clamp using indirect calorimetry and the ventilated hood technique as previously described (5).

Measurement of Metabolites and Hormones. Plasma glucose concentrations were measured with a YSI 2700 STAT Analyzer (Yellow Springs Instruments). Plasma concentrations of insulin, leptin, HMW adiponectin, and C-reactive protein were measured using double-antibody RIA kits (Linco). Plasma fatty acid concentrations were determined by a microfluorometric method (18). Gas chromatography–MS analyses of the APE of [$1\text{-}^{13}\text{C}$] glucose in plasma were measured with a Hewlett–Packard Mass Selective Detector (model 5971A) as previously described (21).

Transmission Electron Microscopy. For electron microscopic examination, individual muscle samples were fixed in 2.5% (vol/vol) glutaraldehyde in 0.1 M cacodylate buffer (pH 7.4) at 4 °C overnight, postfixed in 1% osmium tetroxide in the same buffer for 1 h at room temperature, stained in 2% (wt/vol) uranyl acetate, dehydrated in a graded series of ethanol, and embedded in epoxy resin (Embed-812; Electron Microscopy Sciences). Ultrathin sections (60 nm) were stained with 2% (wt/vol) uranyl acetate and lead citrate and examined in a Tecnai 12 Biotwin electron microscope. Three random sections were examined from each individual muscle, and five random pictures were taken from each section at a magnification of $\times 6,800$ and printed at a final magnification of $\times 18,500$. The volume density of mitochondria was estimated using the point counting method in a blinded fashion. For each set of five pictures, average volume density was calculated, and the mean of three values was used to estimate the volume density for each individual muscle (20, 22).

Akt2 Activity Assay. Basal and insulin-stimulated Akt2 activity in the muscle biopsy samples was assessed in immunoprecipitates by measuring ^{32}P incorporation onto a synthetic Akt substrate as previously described (23).

LC-MS/MS Analyses of ^{13}C Enrichments in Muscle Glutamate and Alanine and Calculations of $V_{\text{PDH}}/V_{\text{CS}}$ Flux. Frozen biopsies (~30–50 mg) were powdered and homogenized in a 50% (vol/vol) acetonitrile solution with 10 μM $^2\text{H}_4$ -taurine, used as loading control. The homogenate was then centrifuged to pellet bulk insoluble materials before filtration (MultiScreen BV; Millipore Corp.). The lysates were separated on a hypercarb column (3- μm particle size, 3 \times 150 mm; Thermo Fisher Scientific) before ionization for multiple reaction monitoring (MRM) analysis by LC-MS/MS (Applied Biosystems MDS SCIEX; 4000 Q-TRAP). Each analyte was eluted isocratically in a mobile phase containing 5% (vol/vol) acetonitrile, 2 mM ammonium acetate, and 10 μM EDTA at a flow rate of 1 mL/min with a single Gaussian-shaped peak of which the retention time was confirmed with known standards.

Individual MRM transition pairs (Q_1/Q_3) were designated for the natural abundance (M) and mass ($M + n$) isotopologues, in which n represents the number of labeled carbons. Alanine enrichments were used as surrogate for pyruvate enrichments, as described previously (9). Alanine was detected in positive mode using the MRM transition pairs (Q_1/Q_3) 90/44 (M), and 91/45 ($M + 1$). The daughter ion $Q_3 = 44$ corresponds to [$2\text{-}^{13}\text{C}$] and [$3\text{-}^{13}\text{C}$] of alanine. The enrichments, in the form of APE, were calculated by the ratio of 91/45 over $\sum(90/44, 91/45)$. Natural abundance of alanine $M + 1$ was calculated from biopsy tissues infused with natural abundance glucose and subtracted from the enriched samples. Given the low APE of alanine $M + 1$, it is assumed that 91/45 corresponds to [$3\text{-}^{13}\text{C}$] alanine and that any recycling of ^{13}C -label through malic enzyme, potentially generating [$2\text{-}^{13}\text{C}$] alanine, is undetectable. Through PDH, [$3\text{-}^{13}\text{C}$] pyruvate is converted to [$2\text{-}^{13}\text{C}$] acetyl-CoA. Total APE in [$4\text{-}^{13}\text{C}$] glutamate was used as a surrogate for [$2\text{-}^{13}\text{C}$] acetyl-CoA

APE. Glutamate was detected using the 146/41 (M) and 147/42 (M + 1) fragments. The daughter ion $Q_3 = 41$ corresponds to glutamate [$4\text{-}^{13}\text{C}$] and [$5\text{-}^{13}\text{C}$] (originated from acetyl-CoA). Therefore, 147/42 corresponds to [$4\text{-}^{13}\text{C}$] glutamate. Glutamate APE was calculated by the ratio of 147/42 over $\sum(147/42, 146/41)$. Glutamate natural abundance was calculated from biopsy tissues infused with natural abundance glucose and subtracted from the enriched samples. The relative $V_{\text{PDH}}/V_{\text{CS}}$ was calculated according to the following formula derived previously (10): $V_{\text{PDH}}/V_{\text{CS}} = [4\text{-}^{13}\text{C}] \text{ glutamate}/[3\text{-}^{13}\text{C}] \text{ alanine}$.

Statistical Analysis. Statistical analyses were performed with StatView software (Abacus Concepts). Statistically significant differences between young control and elderly subjects were detected using unpaired Student *t* tests for

independent samples and the paired Student *t* test for paired samples. All data are expressed as means \pm SE in the text.

ACKNOWLEDGMENTS. We thank Yanna Kosover, Irina Smolgovsky, Mikhail Smolgovsky, Zhen-Xiang Liu, Gina Solomon, RN, and the staff of the Yale-New Haven Hospital Research Unit for expert technical assistance with the studies and the volunteers for participating in this study. This work was supported by National Institutes of Health Grants R01 AG-23686, R01 DK-49230, R01 NS-087568, R24 DK-085638, P30 DK-45735, R01 DK-092606, and M01 RR-00125; the Novo-Nordisk Foundation Center for Basic Metabolic Research; Novartis Pharmaceuticals (K.F.P.); and a Distinguished Clinical Scientist award (to K.F.P.) and a Mentor award (to G.I.S.) from the American Diabetes Association.

1. Basu R, et al. (2003) Mechanisms of the age-associated deterioration in glucose tolerance: Contribution of alterations in insulin secretion, action, and clearance. *Diabetes* 52(7):1738–1748.
2. Harris MI (1993) Undiagnosed NIDDM: Clinical and public health issues. *Diabetes Care* 16(4):642–652.
3. Nesto RW (2003) The relation of insulin resistance syndromes to risk of cardiovascular disease. *Rev Cardiovasc Med* 4(Suppl 6):S11–S18.
4. Short KR, et al. (2005) Decline in skeletal muscle mitochondrial function with aging in humans. *Proc Natl Acad Sci USA* 102(15):5618–5623.
5. Petersen KF, et al. (2003) Mitochondrial dysfunction in the elderly: Possible role in insulin resistance. *Science* 300(5622):1140–1142.
6. Samuel VT, Shulman GI (2012) Mechanisms for insulin resistance: Common threads and missing links. *Cell* 148(5):852–871.
7. Reznick RM, et al. (2007) Aging-associated reductions in AMP-activated protein kinase activity and mitochondrial biogenesis. *Cell Metab* 5(2):151–156.
8. Shulman GI (2014) Ectopic fat in insulin resistance, dyslipidemia, and cardiometabolic disease. *N Engl J Med* 371(12):1131–1141.
9. Lee HY, et al. (2010) Targeted expression of catalase to mitochondria prevents age-associated reductions in mitochondrial function and insulin resistance. *Cell Metab* 12(6):668–674.
10. Alves TC, et al. (2011) Regulation of hepatic fat and glucose oxidation in rats with lipid-induced hepatic insulin resistance. *Hepatology* 53(4):1175–1181.
11. Flannery C, Dufour S, Rabol R, Shulman GI, Petersen KF (2012) Skeletal muscle insulin resistance promotes increased hepatic de novo lipogenesis, hyperlipidemia, and hepatic steatosis in the elderly. *Diabetes* 61(11):2711–2717.
12. Kelley DE, Reilly JP, Veneman T, Mandarino LJ (1990) Effects of insulin on skeletal muscle glucose storage, oxidation, and glycolysis in humans. *Am J Physiol* 258(6 Pt 1):E923–E929.
13. Natali A, et al. (1990) Effects of insulin on hemodynamics and metabolism in human forearm. *Diabetes* 39(4):490–500.
14. Dresner A, et al. (1999) Effects of free fatty acids on glucose transport and IRS-1-associated phosphatidylinositol 3-kinase activity. *J Clin Invest* 103(2):253–259.
15. Cline GW, et al. (1999) Impaired glucose transport as a cause of decreased insulin-stimulated muscle glycogen synthesis in type 2 diabetes. *N Engl J Med* 341(4):240–246.
16. Baecke JA, Burema J, Frijters JE (1982) A short questionnaire for the measurement of habitual physical activity in epidemiological studies. *Am J Clin Nutr* 36(5):936–942.
17. Matsuda M, DeFronzo RA (1999) Insulin sensitivity indices obtained from oral glucose tolerance testing: Comparison with the euglycemic insulin clamp. *Diabetes Care* 22(9):1462–1470.
18. Petersen KF, et al. (2012) Reversal of muscle insulin resistance by weight reduction in young, lean, insulin-resistant offspring of parents with type 2 diabetes. *Proc Natl Acad Sci USA* 109(21):8236–8240.
19. Mayerson AB, et al. (2002) The effects of rosiglitazone on insulin sensitivity, lipolysis, and hepatic and skeletal muscle triglyceride content in patients with type 2 diabetes. *Diabetes* 51(3):797–802.
20. Morino K, et al. (2005) Reduced mitochondrial density and increased IRS-1 serine phosphorylation in muscle of insulin-resistant offspring of type 2 diabetic parents. *J Clin Invest* 115(12):3587–3593.
21. Boumezbeur F, et al. (2010) Altered brain mitochondrial metabolism in healthy aging as assessed by in vivo magnetic resonance spectroscopy. *J Cereb Blood Flow Metab* 30(1):211–221.
22. Zong H, et al. (2002) AMP kinase is required for mitochondrial biogenesis in skeletal muscle in response to chronic energy deprivation. *Proc Natl Acad Sci USA* 99(25):15983–15987.
23. Alessi DR, Caudwell FB, Andjelkovic M, Hemmings BA, Cohen P (1996) Molecular basis for the substrate specificity of protein kinase B; comparison with MAPKAP kinase-1 and p70 S6 kinase. *FEBS Lett* 399(3):333–338.